

Mathematical Model of the Impact of Home-Based Care on Contagious Respiratory Illness Under Optimal Conditions

Henry Milimo Wanjala, Mark O. Okongo, and Jimrise O. Ochwach



Volume 5, Issue 2, Pages 83–94, December 2024

Received 19 September 2024, Revised 12 December 2024, Accepted 19 December 2024, Published Online 30 December 2024

To Cite this Article : H. M. Wanjala, M. O. Okongo, and J. O. Ochwach, "Mathematical Model of the Impact of Home-Based Care on Contagious Respiratory Illness Under Optimal Conditions", *Jambura J. Biomath*, vol. 5, no. 2, pp. 83–94, 2024, <https://doi.org/10.37905/jjbm.v5i2.27611>

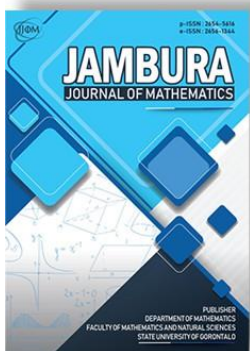
© 2024 by author(s)

JOURNAL INFO • JAMBURA JOURNAL OF BIOMATHEMATICS



Homepage	:	http://ejournal.ung.ac.id/index.php/JJBM/index
Journal Abbreviation	:	Jambura J. Biomath.
Frequency	:	Biannual (June and December)
Publication Language	:	English
DOI	:	https://doi.org/10.37905/jjbm
Online ISSN	:	2723-0317
Editor-in-Chief	:	Hasan S. Panigoro
Publisher	:	Department of Mathematics, Universitas Negeri Gorontalo
Country	:	Indonesia
OAI Address	:	http://ejournal.ung.ac.id/index.php/jjbm/oai
Google Scholar ID	:	XzYgeKQAAAAJ
Email	:	editorial.jjbm@ung.ac.id

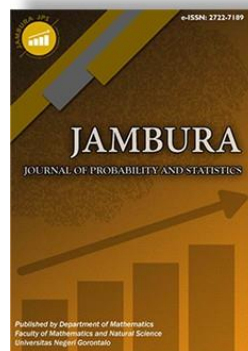
JAMBURA JOURNAL • FIND OUR OTHER JOURNALS



Jambura Journal of Mathematics



Jambura Journal of Mathematics Education




Jambura Journal of Probability and Statistics



EULER : Jurnal Ilmiah Matematika, Sains, dan Teknologi

Mathematical Model of the Impact of Home-Based Care on Contagious Respiratory Illness Under Optimal Conditions

Henry Milimo Wanjala^{1,*} , Mark O. Okongo¹, and Jimrise O. Ochwach²

¹Department of Physical Science, Chuka University, Chuka, Kenya

²Department of Computing and Information Technology, Mama Ngina University College, Gatundu, Kenya

Emails: okongo@chuka.ac.ke

ARTICLE HISTORY

Received 19 September 2024

Revised 12 December 2024

Accepted 19 December 2024

Published 30 December 2024

KEYWORDS

Respiratory Disease
Reproduction Number
Stability Analysis
Home-Based Care
Numerical Simulation
Optimal Control

ABSTRACT. *Mathematical models are vital for understanding real-world phenomena without direct experimentation, particularly in epidemics, as they predict and analyze the effectiveness of various mitigation strategies. Given the rapid transmission of infectious respiratory diseases, public health measures aim to curb spread while managing impacts. This study assesses rapid contact tracing and testing, focusing on isolating confirmed cases through home-based care or traditional methods, on coronavirus transmission within a community. A deterministic mathematical model using ordinary differential equations segments the population into seven compartments: susceptible, exposed, asymptomatic, symptomatic, home-based care, hospitalized, and recovered. The basic reproduction number is determined via the next generation matrix. Local stability of the disease-free equilibrium is analyzed using the trace-determinant method, while global stability is confirmed with the Lyapunov-Krasovskii approach. A Python-based numerical simulation on NumPy and PyPlot uses parameters calibrated to previous studies and estimated for this research. Simulations indicate home-based care delays peak infection days and reduces peak population, providing time to bolster healthcare facilities. Optimal control methods, including media awareness, reduce susceptibility and encourage asymptomatic individuals to choose home-based care. Using Pontryagin's Maximum Principle, the study identifies optimal strategies, highlighting that media awareness effectively lowers susceptibility and optimal control directs asymptomatics to home-based care, reducing strain on healthcare facilities. In conclusion, home-based care is effective for managing mild symptomatic and asymptomatic cases, alleviating pressure on healthcare resources and prioritizing severe cases. Combining home-based care with other non-pharmaceutical strategies is recommended for maximum effectiveness.*



This article is an open access article distributed under the terms and conditions of the Creative Commons Attribution-NonCommercial 4.0 International License. [Editorial of JJBM](#): Department of Mathematics, Universitas Negeri Gorontalo, Jln. Prof. Dr. Ing. B. J. Habiebie, Bone Bolango 96554, Indonesia.

1. Introduction

Our ancestors developed strategies to mitigate the impact of epidemics, which have persisted throughout history, exhibiting varying rates of spread and decline, thus requiring diverse mitigation measures [1]. Respiratory pandemics have caused significant harm to both individuals and societies, necessitating crucial decisions regarding the management of asymptomatic and mildly symptomatic cases within the constraints of healthcare facilities and resources [2, 3]. Due to their active infectious status and higher viral loads, effective management of these cases is essential [2], prompting an examination of the potential role of home-based care in controlling disease transmission.

Monitoring infectious diseases is critical for informing public health interventions. The lack of specific treatment programs for emerging respiratory illnesses, along with vaccine shortages and unequal distribution, highlights the need for rigorous analysis using mathematical models to evaluate management strategies [4]. Predicting the severity and timing of epidemics, as well as minimizing their spread to other regions, are vital considerations [5].

Mathematics has greatly contributed to understanding the

spread and control of emerging and re-emerging infectious diseases. By estimating variations in transmission rates over time, researchers can gain valuable insights into the current epidemiological status and assess the effectiveness of outbreak control measures. This analysis helps predict future trends, evaluate risks to neighboring regions, and develop alternative intervention strategies [6, 7].

In the absence of treatment options and vaccines for new epidemics, identifying effective containment strategies is crucial until pharmaceutical interventions become available [8]. Research, such as that by [9], underscores the importance of non-pharmaceutical measures like social distancing to prevent overwhelming healthcare systems.

The work of [10] identified multiple sources contributing to secondary infections, underscoring the need for precautionary actions. Their study aimed to assess the impact of home-based care on a subset of symptomatic and tested asymptomatic patients. It also investigated the influence of undetected infected individuals on transmission dynamics and analyzes the effects of reduced infection rates in isolated patients.

Overall, implementing a comprehensive suite of interventions would be most effective in controlling COVID-19 outbreaks,

*Corresponding Author.

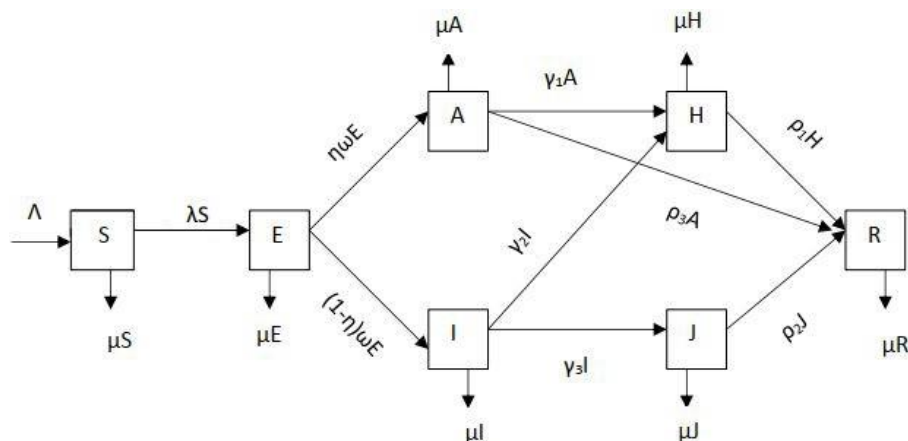


Figure 1. Model Flow Chart

though it would inevitably result in increased economic and social costs [11].

This study aims to develop and analyze a mathematical model that examines how isolation through home-based care impacts the spread of respiratory infectious diseases. It also investigates the role of hospitalization in reducing disease transmission. Together, these strategies are assessed for their effectiveness in controlling the outbreak.

2. Model Formulation and Development

The population is divided into seven distinct groups: susceptible ($S(t)$), exposed ($E(t)$), asymptomatic ($A(t)$), symptomatic ($I(t)$), those under home-based care ($H(t)$), isolated ($J(t)$), and the recovered ($R(t)$). Initially, all individuals entering the population are susceptible at a rate denoted by Λ . Susceptible individuals become exposed at a rate of λ , where the effective contact rate is represented by β . After an incubation period of ω , a portion of the exposed population, denoted by η , becomes asymptomatic, while the remainder develop symptoms. Asymptomatic individuals identified through contact tracing are placed under home-based care at a rate of γ_1 and recover at a rate of ρ_1 . Those asymptomatic individuals not identified through contact tracing recover naturally at a rate of ρ_3 . Symptomatic individuals may either be hospitalized at a rate of γ_3 if their condition worsens or placed under home-based care at a rate of γ_2 . Hospitalized individuals recover at a rate of ρ_2 . Infections primarily occur through interactions with symptomatic individuals who do not take precautionary measures. The infectivity of the exposed population under home-based care is reduced by factors denoted as $\epsilon_4, \epsilon_2, \epsilon_1$, and ϵ_3 respectively. Additionally, a natural death rate of μ applies across all compartments. The model flow chart is shown in Figure 1. The model equations are represented in eq. (1)

$$\begin{aligned} \frac{dS}{dt} &= \Lambda - (\lambda + \mu)S, \\ \frac{dE}{dt} &= \lambda S - (\mu + \omega)E, \\ \frac{dA}{dt} &= \eta\omega E - (\mu + \rho_3 + \gamma_1)A, \\ \frac{dI}{dt} &= (1 - \eta)\omega E - (\mu + \gamma_2 + \gamma_3)I, \end{aligned}$$

$$\begin{aligned} \frac{dH}{dt} &= \gamma_1 A + \gamma_2 I - (\rho_1 + \mu)H, \\ \frac{dJ}{dt} &= \gamma_3 I - (\mu + \rho_2)J, \\ \frac{dR}{dt} &= \rho_1 H + \rho_2 J + \rho_3 A - \mu R. \end{aligned} \tag{1}$$

The force of infection, λ is given by eq. (2):

$$\lambda = \frac{\beta(A + \epsilon_1 I + \epsilon_2 H + \epsilon_3 J + \epsilon_4 E)}{N} \tag{2}$$

The model parameters and the parameter values are shown in the Table 1 below

3. Model Analysis

3.1. Positivity of the Solution

The model (1) deals with living organisms and thus the associated state variables are non-negative for all the time $t > 0$. Thus, the solutions to model (1) with initial data is positive for all time $t > 0$.

Theorem 1. The region

$$D = \{ (S(t), E(t), A(t), I(t), H(t), J(t), R(t)) \in \mathbb{R}_+^7 : N(t) \leq \frac{\Lambda}{\mu} \}$$

is positively invariant and attracting with respect to model (1).

Proof. Solving the first equation of 1 for $S(t)$ at time, $t > 0$, it is obtained that:

$$\begin{aligned} \frac{dS}{dt} &= \Lambda - (\lambda + \mu)S, \\ \frac{dS}{dt} &\geq -(\lambda + \mu)S, \\ \int_s \frac{dS}{S} &\geq -(\lambda + \mu)dt, \\ \int_{s(0)}^s \frac{dS}{S} &\geq -(\lambda + \mu)dt, \\ \ln S - \ln S(0) &\geq -(\lambda + \mu)dt, \\ \ln \frac{S}{S(0)} &\geq -(\lambda + \mu)dt, \end{aligned}$$

Table 1. Parameter values

Symbol	Parameter	Value	Source
Λ	Recruitment rate by birth	0.00018 days ⁻¹	[12]
μ	Natural death rate	4.563 × 10 ⁻⁵ days ⁻¹	[12]
ρ_1	Rate of recovery of home-based care patients	0.0714	[13]
ρ_2	Rate of recovery of hospitalised patients	0.2992	[14]
ρ_3	Rate of recovery of asymptomatic patients	0.98	[13]
ω	Latency period	1/10	Assumed
γ_1	rate of transfer of A to H	0.1168	[15]
γ_2	rate of transfer of I to H	0.98	[10]
γ_3	rate of hospitalisation of symptomatic patients	0.33604	[16]
β	Effective contact rate	0.5 days ⁻¹	[17]
ϵ_1	Infections by the Symptomatics	0.0405	[10]
ϵ_2	infections by those under Home - based care	0.0175	[10]
ϵ_3	infections by the Hospitalised	0.0050	[10]
ϵ_4	infections by the Hospitalised	0.0050	Assumed
η	Fraction of those Asymptomatic but Infectious	0.7	[10]

$$\frac{S}{S(0)} \geq e^{-\int (\lambda+\mu)dt},$$

$$S \geq S(0)e^{-\int (\lambda+\mu)dt}.$$

Clearly, $S(0) e^{-\int (\lambda+\mu)dt}$ is a non-negative function of t , thus $S(t)$ stays positive.

Equivalent demonstrations can be constructed to affirm the positivity of various variables by employing the relevant equations within the system. This implies that the solutions to model (1), given non-negative initial conditions such that $E(t) > 0, A(t) > 0, I(t) > 0, H(t) > 0, J(t) > 0$, and $R(t) > 0$, will persist in non-negativity for all time instances $t \geq 0$. □

3.2. Invariant Region

Theorem 2. *There exists a domain H in which the solution set $\{S(t), E(t), A(t), I(t), H(t), J(t), \text{ and } R(t)\}$ of model (1) is positively invariant.*

Proof. The total human population can be determined by,

$$N(t) = S(t) + E(t) + A(t) + I(t) + H(t) + J(t) + R(t).$$

Then the time derivatives of $N(t)$ along the solutions of model (1) gives the following:

$$\frac{dN}{dt} = \Lambda - \mu N. \tag{3}$$

In the absence of the disease, in the population,

$$\frac{dN}{dt} \leq \Lambda - \mu N \Rightarrow N(t) = \frac{\Lambda}{\mu} + N(0) - \frac{\Lambda}{\mu} e^{-\mu t},$$

$$N(0) = S(0) + E(0) + A(0) + S(0) + h(0) + J(0) + R(0).$$

Thus, if $N(0) \leq \frac{\Lambda}{\mu}$, then $N(t) \leq \frac{\Lambda}{\mu}$ as $t \rightarrow \infty$. Therefore,

$$H = \left\{ (S(t), E(t), IA(t), I(t), H(t), J(t), R(t)) \in \mathbb{R}^7 : N(t) \leq \frac{\Lambda}{\mu} \right\}$$

is the feasible solution of model (1) which implies the total number of human population is positively invariant. Therefore, the model is biologically meaningful and mathematically well posed in the region H □

3.3. Basic Reproduction Number

The basic reproduction number (R_0) serves as a gauge for the number of new infections generated by an index patient within a population that is entirely susceptible.

The basic reproduction number, R_0 , is derived through the utilisation of the Next Generation Matrix (NGM). The Jacobian matrix, derived from the equations of the model, is instrumental in computing this reproduction number.

Theorem 3. *The basic reproduction number (R_0) for the epidemiological model (1) is given by eq. (4):*

$$R_0 = \frac{m\beta k_4}{k_1 k_2} + \frac{m\beta(1-\eta)\omega\epsilon_1}{k_1 k_3} + \frac{m\beta\gamma_3\epsilon_3}{k_1 k_3 k_5} + \frac{m\beta\epsilon_4}{k_4} + \frac{m\beta\omega\epsilon_2(\eta\gamma_1 k_3 k_4 + (1-\eta)\gamma_2 k_2)}{k_2 k_3 k_5} \tag{4}$$

where: $m = \frac{\Lambda}{\mu}$, $k_1 = (\mu + \omega)$, $k_2 = (\mu + \gamma_1 + \rho_3)$, $k_3 = (\mu + \gamma_2 + \gamma_3)$, $k_4 = (\mu + \rho_1)$, and $k_5 = (\mu + \rho_2)$.

Proof. The basic reproduction number can be defined as the spectral radius of the matrix product FV^{-1} . To obtain this, we isolate the infectious subsystem from the model (1) and derive the transmission matrix (F) and the transition matrix (V) as outlined in eqs. (5) and (6):

$$F = \begin{pmatrix} m\beta\epsilon_4 & m\beta & m\beta\epsilon_1 & m\beta\epsilon_2 & m\beta\epsilon_3 \\ 0 & 0 & 0 & 0 & 0 \\ 0 & 0 & 0 & 0 & 0 \\ 0 & 0 & 0 & 0 & 0 \\ 0 & 0 & 0 & 0 & 0 \end{pmatrix}, \tag{5}$$

$$V = \begin{pmatrix} -k_1 & 0 & 0 & 0 & 0 \\ \eta\omega & -k_2 & 0 & 0 & 0 \\ (1-\eta)\omega & 0 & -k_3 & 0 & 0 \\ 0 & \gamma_1 & \gamma_2 & -k_4 & 0 \\ 0 & 0 & \gamma_3 & 0 & -k_5 \end{pmatrix}, \tag{6}$$

and we have

$$FV^{-1} = \begin{bmatrix} R_0 & -I_1 & -I_2 & -I_3 & -I_4 \\ 0 & 0 & 0 & 0 & 0 \\ 0 & 0 & 0 & 0 & 0 \\ 0 & 0 & 0 & 0 & 0 \\ 0 & 0 & 0 & 0 & 0 \end{bmatrix},$$

$$I_1 = \frac{m\beta\epsilon_2\gamma_1 + m\beta k_4}{k_4},$$

$$I_2 = \frac{m\beta\epsilon_2 k_5 + k_4(k_5 m\beta\epsilon_1 + m\beta\epsilon_3 \gamma_3)}{k_3 k_4 k_5},$$

$$I_3 = \frac{m\beta\epsilon_2}{k_4},$$

$$I_4 = \frac{m\beta\epsilon_3}{k_5}.$$

Thus, the basic reproduction equation is given by

$$R_0 = \frac{m\beta k_4}{k_1 k_2} + \frac{m\beta(1-\eta)\omega\epsilon_1}{k_1 k_3} + \frac{m\beta\gamma_3\epsilon_3}{k_1 k_3 k_5} + \frac{m\beta\epsilon_4}{k_4} + \frac{m\beta\omega\epsilon_2(\eta\gamma_1 k_3 k_4 + (1-\eta)\gamma_2 k_2)}{k_2 k_3 k_5}.$$

3.4. Equilibrium Analysis

1. Disease Free Equilibrium Point

The Disease-Free Equilibrium (DFE) for model (1) is reached when all the classes related to infection are set to zero, leading to the formulation of eq. (7):

$$E^* = (S^0, E^0, H^0, A^0, I^0, J^0, R^0),$$

$$E^* = \left(\frac{\Delta}{\mu}, 0, 0, 0, 0, 0, 0 \right).$$

2. Stability Analysis of the Disease Free Equilibrium Point

[18] presented a theorem for conducting local stability analysis of a system of ordinary differential equations using numerical methods.

Theorem 4. Assume the first order partial derivatives of f and g are continuous in some open set containing the equilibrium point (\hat{x}, \hat{y}) . Then, the equilibrium is locally asymptotically stable if,

- i. $Tr(J) < 0$, and
- ii. $\det(J) > 0$

where, J is the Jacobian matrix evaluated at the equilibrium. In addition, the equilibrium is unstable if either $Tr(J) > 0$ or $\det(J) < 0$.

Computing the Jacobian matrix of eq. (1) at DFE, it yields eq. (8):

$$J_f = \begin{bmatrix} k_1 & m\beta\epsilon_4 & m\beta & m\beta\epsilon_1 & m\beta\epsilon_2 & m\beta\epsilon_3 & 0 \\ 0 & k_2 + m\beta\epsilon_4 & m\beta & m\beta\epsilon_1 & m\beta\epsilon_2 & m\beta\epsilon_3 & 0 \\ 0 & \eta\omega & k_3 & 0 & 0 & 0 & 0 \\ 0 & (1-\eta)\omega & 0 & k_4 & 0 & 0 & 0 \\ 0 & 0 & \gamma_1 & \gamma_2 & k_5 & 0 & 0 \\ 0 & 0 & 0 & \gamma_3 & 0 & k_6 & 0 \\ 0 & 0 & \rho_3 & 0 & \rho_1 & \rho_3 & k_7 \end{bmatrix},$$

Where: $k_1 = -\mu$, $k_2 = -(\mu + \omega)$, $k_3 = -(\mu + \gamma_1 + \epsilon_3)$, $k_4 = -(\mu + \gamma_2 + \gamma_3)$, $k_5 = -(\mu + \rho_1)$, $k_6 = -(\mu + \rho_2)$, $k_7 = -\mu$, and $m = \frac{\Delta}{\mu}$. Based on matrix (8) and numerical parameter substitution, it is concluded that:

- i. $Tr(J_f) < 0$, and
- ii. $\det(J_f) > 0$

Thus, the DFE is locally asymptotically stable. This findings are in line with the findings of [19].

3. Global Stability Analysis of the DFE

We employ the Lyapunov-Krasovskii method for analysing the global asymptotic stability.

Theorem 5. Consider the autonomous system defined by $\hat{x} = f(x)$, with the equilibrium point of interest being the origin. Let $A(x)$ denote the Jacobian matrix of the system, $A(x) = \frac{\partial f}{\partial x}$. If the matrix $F = A + A^T$ is negative neighborhood Ω , then, the equilibrium point at the origin is asymptotically stable. A Lyapunov function for this system is

$$V(x) = f^T(x)f(x). \tag{9}$$

If Ω is the entire state space and, in addition, $V(x) \rightarrow \infty$, $\|x\| \rightarrow \infty$, then, the equilibrium point is said to be globally asymptotically stable.

The global stability analysis is performed by constructing the Jacobian matrix of the model (1) and solving it at the DFE as shown in matrix (10).

$$F(x) = \begin{bmatrix} k_1 & m\beta\epsilon_4 & m\beta & m\beta\epsilon_1 & m\beta\epsilon_2 & m\beta\epsilon_3 & 0 \\ 0 & k_2 + m\beta\epsilon_4 & m\beta & m\beta\epsilon_1 & m\beta\epsilon_2 & m\beta\epsilon_3 & 0 \\ 0 & \eta\omega & k_3 & 0 & 0 & 0 & 0 \\ 0 & (1-\eta)\omega & 0 & k_4 & 0 & 0 & 0 \\ 0 & 0 & \gamma_1 & \gamma_2 & k_5 & 0 & 0 \\ 0 & 0 & 0 & \gamma_3 & 0 & k_6 & 0 \\ 0 & 0 & \rho_3 & 0 & \rho_1 & \rho_3 & k_7 \end{bmatrix},$$

where: $k_1 = -(\mu)$, $k_2 = -(\mu + \omega)$, $k_3 = -(\mu + \gamma_1 + \epsilon_3)$, $k_4 = -(\mu + \gamma_2 + \gamma_3)$, $k_5 = -(\mu + \rho_1)$, $k_6 = -(\mu + \rho_2)$, $k_7 = -(\mu)$, and $m = \frac{\Delta}{\mu}$.

From the matrix (10) above, the transpose ($F^T(x)$) of $F(x)$ is as shown in matrix (11):

$$F^T(x) = \begin{bmatrix} k_1 & 0 & 0 & 0 & 0 & 0 & 0 \\ 0 & k_2 + m\beta\epsilon_4 & \eta\omega & (1-\eta)\omega & 0 & 0 & 0 \\ -m\beta & m\beta & k_3 & 0 & \gamma_1 & 0 & \rho_3 \\ -m\beta\epsilon_1 & m\beta\epsilon_4 & 0 & k_4 & \gamma_2 & \gamma_3 & 0 \\ -m\beta\epsilon_2 & m\beta\epsilon_2 & 0 & 0 & k_5 & 0 & \rho_1 \\ -m\beta\epsilon_3 & m\beta\epsilon_3 & 0 & 0 & 0 & k_6 & \rho_2 \\ 0 & 0 & 0 & 0 & 0 & 0 & k_7 \end{bmatrix},$$

where: $k_1 = -(\mu)$, $k_2 = -(\mu + \omega)$, $k_3 = -(\mu + \gamma_1 + \epsilon_3)$, $k_4 = -(\mu + \gamma_2 + \gamma_3)$, $k_5 = -(\mu + \rho_1)$, $k_6 = -(\mu + \rho_2)$, $k_7 = -(\mu)$, and $m = \frac{\Delta}{\mu}$.

From the matrix above, $\hat{F}(x)$ is as follows:

$$\hat{F}(x) = F^T(x) + F(x).$$

This implies that $\hat{F}(x)$ is as in matrix (12):

$$\hat{F}(x) = \begin{bmatrix} F_{11} & F_{12} & F_{13} & F_{14} & F_{15} & F_{16} & 0 \\ F_{21} & F_{22} & F_{23} & F_{24} & F_{25} & F_{26} & 0 \\ F_{31} & F_{32} & F_{33} & 0 & F_{35} & 0 & F_{37} \\ F_{41} & F_{42} & 0 & F_{44} & F_{45} & F_{46} & 0 \\ F_{51} & F_{52} & F_{53} & F_{54} & F_{55} & 0 & 0 \\ F_{61} & F_{62} & 0 & F_{64} & 0 & F_{66} & F_{67} \\ 0 & 0 & F_{73} & 0 & F_{75} & F_{76} & F_{77} \end{bmatrix}, \tag{12}$$

where

$$\begin{aligned} F_{11} &= 2k_1, & F_{12} &= -m\theta\epsilon_4, & F_{13} &= -m\theta, \\ F_{14} &= -m\theta\epsilon_1, & F_{15} &= -m\theta\epsilon_2, & F_{16} &= -m\theta\epsilon_4, \\ F_{21} &= -m\theta\epsilon_4, & F_{22} &= 2k_2 + 2m\theta\epsilon_4, & F_{23} &= m\theta + \eta\omega, \\ F_{24} &= (1 - \eta)\omega + \epsilon_1 m\theta, & F_{25} &= \epsilon_2 m\theta, & F_{26} &= \epsilon_3 m\theta, \\ F_{31} &= -m\theta, & F_{32} &= \eta\omega + m\theta, & F_{33} &= 2k_3, \\ F_{35} &= \nu_1, & F_{37} &= \rho_3, & F_{41} &= -m\theta\epsilon_1, \\ F_{42} &= (1 - \eta)\omega + m\theta\epsilon_1, & F_{44} &= 2k_4, & F_{45} &= \nu_2, \\ F_{46} &= \nu_3, & F_{51} &= -m\theta\epsilon_2, & F_{52} &= m\theta\epsilon_2, \\ F_{53} &= \nu_1, & F_{54} &= \nu_2, & F_{55} &= 2k_5, \\ F_{61} &= -m\theta\epsilon_3, & F_{62} &= m\theta\epsilon_3, & F_{64} &= \nu_3, \\ F_{66} &= 2k_6, & F_{67} &= \rho_2, & F_{73} &= \rho_3, \\ F_{75} &= \rho_1, & F_{76} &= \rho_2, & F_{77} &= 2k_7. \end{aligned}$$

The matrix $\hat{F}(x)$ is to be checked if it is negative definite. This is by getting the principal determinants of the matrix $\hat{F}(x)$

- i. $2k_1$ is negative definite, and
- ii. $\det(\hat{F}(x))$ is negative definite.

So, the matrix $\hat{F}(x)$ is negative definite. This, is a Lyapunov function for the system $F(x)$, and, thus,

$$V(x) = f^T(x)f(x).$$

If Ω is the entire state space and, in addition, $V(x) \rightarrow \infty$, $\|x\| > \infty$, then the equilibrium point is said to be globally asymptotically stable as illustrated by [20].

4. Bifurcation Analysis

Bifurcation analysis is critical in identifying parameter values or thresholds where qualitative changes in the system's behaviour occur. The changes can signify transitions between disease free states, endemic states and even periodic outbreaks. These thresholds are crucial for predicting and controlling disease dynamics.

Theorem 6. Theorem 4.1 of [25]. Consider the following general system of ordinary differential equations with a parameter ϕ .

$$\frac{dx}{dt} = f(x, \phi), f: \mathbb{R}^n \times \mathbb{R} \rightarrow \mathbb{R} \text{ and } f \in C^2(\mathbb{R}^n \times \mathbb{R}) \tag{13}$$

Where 0 is an equilibrium point of the system (that is, $f(0, \phi) = 0, \forall \phi$) and assume

- $A = D_x f(0, 0) = \left[\frac{\partial f_i}{\partial x_j}(0, 0) \right]$ is the linearization matrix of 2.1 around the equilibrium point 0 with ϕ evaluated at 0 , zero is a simple eigenvalue of A and other eigenvalues of A have negative real parts.
- Matrix A has a right eigenvector w and left eigenvector v

(each corresponding to zero eigenvalues)

Let f_k be k -th component of f and

$$\begin{aligned} a &= \sum_{k,i,j=1}^n v_k w_i w_j \frac{\partial^2 f_k}{\partial x_i \partial x_j}(0, 0), \\ b &= \sum_{k,i=1}^n v_k w_i \frac{\partial^2 f_k}{\partial x_i \partial \phi}(0, 0). \end{aligned}$$

The local dynamics of the system (13) around 0 is totally determined by the signs of a and b .

- (i) $a > 0, b > 0$, when $\phi < 0$ with $|\phi| \ll 1$, 0 is locally asymptotically stable and there exists a positive unstable equilibrium; when $0 < \phi \ll 1$, 0 is unstable and there exist a negative and locally asymptotically stable equilibrium.
- (ii) $a < 0, b < 0$. When $\phi < 0$ with $|\phi| \ll 1$, 0 is locally asymptotically stable and there exists a positive unstable equilibrium; when $0 < \phi \ll 1$, 0 is unstable and there exist a positive unstable equilibrium.
- (iii) $a > 0, b < 0$, when $\phi < 0$ with $|\phi| \ll 1$, 0 is unstable, and there exists a locally asymptotically stable negative equilibrium; when $0 < \phi \ll 1$, 0 is stable, and a positive unstable equilibrium appears.
- (iv) $a < 0, b > 0$. When ϕ changes from negative to positive, 0 changes its stability from stable to unstable. Correspondingly a negative unstable equilibrium becomes positive and locally asymptotically stable.

Let the model (1) be written in the vector form:

$$\frac{dx}{dt} = G(x),$$

where

$$\begin{aligned} X &= (x_1, x_2, x_3, x_4, x_5, x_6, x_7)^T, \\ G &= (g_1, g_2, g_3, g_4, g_5, g_6, g_7), \end{aligned}$$

so that $S = x_1, E = x_2, A = x_3, I = x_4, H = x_5, J = x_6$, and $R = x_7$. Then model (1) becomes as in eq. (14):

$$\begin{aligned} \frac{dx_1}{dt} &= \Lambda - (\lambda + \mu)x_1, \\ \frac{dx_2}{dt} &= \lambda x_1 - (\mu + \omega)x_2, \\ \frac{dx_3}{dt} &= \eta\omega x_2 - (\mu + \rho_3 + \nu_1)x_3, \\ \frac{dx_4}{dt} &= (1 - \eta)\omega x_2 - (\mu + \nu_2 + \nu_3)x_4, \\ \frac{dx_5}{dt} &= \nu_1 x_3 + \nu_2 I - (\rho_1 + \mu)x_5, \\ \frac{dx_6}{dt} &= \nu_3 x_4 - (\mu + \rho_2)x_6, \\ \frac{dx_7}{dt} &= \rho_1 x_5 + \rho_2 x_6 + \rho_3 x_3 - \mu x_7. \end{aligned} \tag{14}$$

Let β be the bifurcation parameter, then $R_0 = 1$ in eq. (4) and

solving for β yields:

$$\beta = \hat{\beta} = \frac{k_1 k_2}{m k_4} + \frac{k_1 k_3}{m(1-\eta)\omega\epsilon_1} + \frac{k_1 k_3 k_5}{m \gamma_3 \epsilon_3} + \frac{k_4}{m \epsilon_4} + \frac{k_2 k_3 k_5}{m \omega \epsilon_2 (\eta \gamma_1 k_1 k_3 + (1-\eta) \gamma_2 k_2 k_4)} \tag{15}$$

So that the disease-free equilibrium, E_0 , is locally stable when $\beta < \hat{\beta}$, and is unstable when $\beta > \hat{\beta}$. Therefore, $\hat{\beta}$ is the bifurcation value.

The linearized matrix of model (1) around the disease-free equilibrium, E_0 , and evaluated at $\hat{\beta}$ is given by:

$$J(E_0|\hat{\beta}) = \begin{bmatrix} k_1 & -a_1 & -a_2 & -a_3 & -a_4 & -a_4 & 0 \\ 0 & a_1 + k_2 & a_2 & a_3 & a_4 & a_5 & 0 \\ 0 & \omega\eta & k_3 & 0 & 0 & 0 & 0 \\ 0 & (1-\omega)\eta & 0 & k_4 & 0 & 0 & 0 \\ 0 & 0 & \gamma_1 & \gamma_2 & k_5 & 0 & 0 \\ 0 & 0 & 0 & \gamma_3 & 0 & k_6 & 0 \\ 0 & 0 & \rho_3 & 0 & \rho_1 & \rho_1 & k_7 \end{bmatrix} \tag{16}$$

where $k_1 = -\mu$, $k_2 = -(\omega + \mu)$, $k_3 = -(\mu + \rho_3 + \gamma_1)$, $k_4 = -(\mu + \gamma_2 + \gamma_3)$, $k_5 = -(\mu + \rho_1)$, $k_6 = -(\mu + \rho_2)$, $k_7 = -\mu$, $a_1 = m\beta\epsilon_1$, $a_2 = m\beta$, $a_3 = m\beta\epsilon_1$, $a_4 = m\beta\epsilon_2$, and $a_5 = m\beta\epsilon_3$.

The eigenvalues are six which are real and negative except zero eigenvalues, which can be obtained by Wolfram Mathematica software as $k_1, k_2, k_3, k_4, k_5, k_6, k_7$. The zero is a simple eigen value of the Jacobian matrix $J(E_0|\hat{\beta})$ and the eigen values are equal and negative. Therefore, the DFE, E_0 is a non-hyperbolic equilibrium, which is in line with the assumption in Theorem 4.1 of [25].

As a result, the centre manifold theory can be applied to determine the local stability of DFE point, E_0 . The right eigen vector, $m = (m_1, m_2, m_3, m_4, m_5, m_6, m_7)^T$ and left eigenvector, $v = (v_1, v_2, v_3, v_4, v_5, v_6, v_7)$ associated with this simple zero eigen eigenvalues of the matrix $J(E_0|\hat{\beta})$ such the $v \cdot m = 1$, can be obtained by multiplying vJ and mJ and setting each of them equal to zero. The resulting system of the right eigenvalues become;

$$\begin{aligned} m_1 k_1 - m_2 a_1 - m_3 a_2 - m_4 a_3 - m_5 a_4 - m_6 a_5 &= 0, \\ m_2 b_1 + m_3 a_2 + m_4 a_2 + m_5 a_4 + m_6 a_5 &= 0, \\ \eta \omega m_2 + m_3 k_3 &= 0, \\ (1-\eta)\omega m_2 + m_4 k_4 &= 0, \\ m_3 \gamma_1 + m_4 \gamma_2 + m_5 k_5 &= 0, \\ m_4 \gamma_3 + m_6 k_6 &= 0, \\ m_3 \rho_3 + m_5 \rho_1 + m_6 \rho_2 + m_7 k_7 &= 0. \end{aligned} \tag{17}$$

From the eq. (17) above, let $m_2 = m_2 > 0$, then;

$$\begin{aligned} m_3 &= \frac{-\eta \omega m_2}{k_3}, \\ m_4 &= \frac{-(1-\eta)\omega m_2}{k_4}, \\ m_5 &= \frac{-(\gamma_1 m_3 + \gamma_2 m_4)}{k_5}, \end{aligned} \tag{18}$$

$$\begin{aligned} m_6 &= \frac{-\gamma_2 m_4}{k_5}, \\ m_6 &= \frac{m_3 \rho_3 + m_5 \rho_1 + m_6 \rho_2}{k_7}, \\ m_1 &= \frac{1}{k_1} (m_2 a_1 + m_3 a_2 + m_4 a_3 + m_5 a_4 + m_6 a_5). \end{aligned} \tag{19}$$

Also, the left eigenvector $v = (v_1, v_2, v_3, v_4, v_5, v_6, v_7)$ corresponding to the zero eigenvalue is obtained from $J(E_0|\hat{\beta})v = 0$ which yields;

$$\begin{aligned} v_1 k_1 &= 0, \\ -v_1 a_1 + v_2 b_1 + v_3 \eta \omega + v_4 (1-\eta)\omega &= 0, \\ -v_1 a_2 + v_2 a_2 + v_3 k_3 + v_4 \gamma_1 + v_5 + v_6 \rho_3 &= 0, \\ -v_1 a_3 + v_2 a_3 + v_4 k_4 + v_5 \gamma_2 + v_6 \gamma_3 &= 0, \\ -v_1 a_4 + v_2 a_4 + v_5 k_5 + v_7 \rho_1 &= 0, \\ -v_1 a_5 + v_2 a_5 + v_3 k_6 + v_4 \rho_2 &= 0, \\ v_7 k_7 &= 0. \end{aligned} \tag{20}$$

From eq. (20) above, $v_1 = v_7 = 0$; then; let, $v_2 = v_2 > 0$, then;

$$\begin{aligned} v_6 &= \frac{-a_5 v_2}{k_6}, \\ v_5 &= \frac{-a_3 v_2}{a_2}, \\ v_3 &= \frac{-(a_2 v_2 + v_1 v_5)}{k_3}, \\ v_4 &= -\frac{v_2 a_3 + v_5 \gamma_2 + v_6 \gamma_3}{k_4}. \end{aligned} \tag{21}$$

To satisfy the condition $v \cdot m = 1$, we determine the value of v_2 . To compute the bifurcation coefficients a and b as defined in Theorem 4.1, we consider model (1) in the following form:

$$\frac{dX}{dt} = f = (f_1, f_2, f_3, f_4, f_5, f_6, f_7)^T, \tag{22}$$

where $X = (x_1, x_2, x_3, x_4, x_5, x_6, x_7)^T$.

The coefficients a and b are derived from the partial derivatives in eq. (23), respectively.

$$\begin{aligned} a &= \sum_{k,i,j=1} v_k m_i m_j \frac{\partial^2 f_k}{\partial x_i \partial x_j} (0, 0), \\ b &= \sum_{k,i=1} v_k m_i \frac{\partial^2 f_k}{\partial x_i \partial \xi} (0, 0). \end{aligned} \tag{23}$$

Since the components of v_1, v_7 are zero we do not need to find the derivatives of f_1, f_7 . From the derivative of the remaining f_2, f_3, f_4, f_5, f_6 , the only ones that have non-zero partial derivatives are considered such that:

$$\begin{aligned} \frac{\partial^2 f_2}{\partial x_1 \partial x_2} &= \frac{\partial^2 f_2}{\partial x_2 \partial x_1} = \epsilon_4, & \frac{\partial^2 f_2}{\partial x_1 \partial x_3} &= \frac{\partial^2 f_2}{\partial x_3 \partial x_1} = 1, \\ \frac{\partial^2 f_2}{\partial x_1 \partial x_4} &= \frac{\partial^2 f_2}{\partial x_4 \partial x_1} = \epsilon_1, & \frac{\partial^2 f_2}{\partial x_1 \partial x_5} &= \frac{\partial^2 f_2}{\partial x_5 \partial x_1} = \epsilon_2, \\ \frac{\partial^2 f_2}{\partial x_1 \partial x_6} &= \frac{\partial^2 f_2}{\partial x_6 \partial x_1} = \epsilon_1. \end{aligned} \tag{24}$$

Considering, the study of [26], the indication of either having a forward or backward bifurcation is determined by α . Consequently, it yields eq. (25):

$$\alpha = 2v_1m_1m_4\epsilon_4 + 2v_3m_1m_3 + 2v_4m_1m_4\epsilon_1 + 2v_5m_1m_5\epsilon_2 + 2v_6m_1m_6\epsilon_3 > 0. \tag{25}$$

Therefore, a mathematical system consisting of equations as presented in eq. (1) exhibits a retrograde bifurcation at $R^* = 1$, given that $\beta > \hat{\beta}$ (representing the effective contact rate). This suggests that the complete elimination of the virus cannot be definitively achieved solely by ensuring that $R^* < 0$. There exists a potential scenario where a resurgence of the epidemic might occur at a later time.

5. Numerical Simulation

To understand the effects of various interventions in preventing and managing COVID-19, a numerical simulation of system model (1) is conducted. The model incorporates parameter values from existing studies, with some values estimated to facilitate a meaningful analysis for this study.

For this investigation, we utilised the parameter values outlined in Table 1 for numerical simulations. The simulations were conducted over the time span of $0 \leq t \leq 100$ days, representing the anticipated duration for the disease to run its course. Python software, with Jupyter serving as the integrated development environment (IDE), was employed to conduct the simulations. The outcomes are depicted graphically.

5.1. Numerical Simulation on the Impact of Isolation

Figure 2 depicts the simulation of infections in the absence of interventions. The symptomatic population rises and becomes entrenched within the community. Due to their lengthier recovery period relative to asymptomatic cases, the overall population is higher. Implementation of interventions such as isolation via hospitalisation and home-based care extends the peak time while notably reducing the peak population, as demonstrated in Figure 3. The implementation of the interventions gives the time for the public health officials to implement a more robust action plan. The imperative for interventions is evident whenever infections occur.

5.2. Numerical Simulation on Impact of Home-based Care

Community mitigation strategies such as home-based care become imperative in the initial stages of an epidemic or when the standard treatment protocol is unavailable. Implementing robust contact tracing measures is crucial to isolate the maximum fraction of infected individuals, including asymptomatic cases. Redirecting individuals with mild symptoms to home-based care instead of hospitalisation is essential to alleviate strain on hospital bed capacity. It also relieves the burden on the health professionals on the number of the patients to attend to reducing fatigue.

Figure 4 demonstrates the impact of home-based care on the asymptomatic population. Numerical simulations reveal that increasing the transfer rate of asymptomatic patients from 10% to 50% results in a decrease in the asymptomatic population from 57 to 34. Further increasing the transfer rate to 90% reduces the

population to 24. Although the peak day shifts from the 31st to the 30th day, the overall scenario remains consistent when considering symptomatic cases.

Similarly, increasing the home-based care rate from 10% to 50% lowers the symptomatic population from 33 patients to 18, shifting the peak day from the 32nd to the 31st day. Further increasing the rate to 90% reduces the population to 12, as depicted in Figure 5.

5.3. Numerical Simulation on Impact of Hospitalisation

Hospitalisation of the symptomatic patients is important in the altering the spread of the disease. When the rate of hospitalisation is increased from 10% to 50% the symptomatic patients are lowered from 14 to 10 patients with also lowering the peak day from the 31st day to the 30th day as illustrated by Figure 6. When the rate of hospitalisation is increased to 90% the patients are 7.

6. Extension of the Model into Optimal Control

In this section, we explore the optimal control of model (1), which characterises the interaction of the level of effectiveness of the media coverage and the application of the home based care to the asymptomatic patients. The primary objective of optimal control is to reduce the total number of infected individuals while minimising the associated costs. We apply optimal control to model (1) to examine the effects of implementing continuous media awareness and vaccination strategies to curb the COVID-19 outbreak. To achieve this, we introduce a set of time-dependent control variables, $u_1(t)$ and $u_2(t)$, where:

1. $u_1(t)$ represents efforts directed towards raising awareness among susceptible individuals through various media outlets.
2. $u_2(t)$ represents efforts aimed at promoting the continuous vaccination of susceptible individuals.

For simplicity, we denote $u_1(t)$ as u_1 and $u_2(t)$ as u_2 . By incorporating these intervention strategies into model (1), we obtain an optimal control model described by eq. (26):

$$\begin{aligned} \frac{dS}{dt} &= \Lambda - (\lambda + \mu + u_1)S, \\ \frac{dE}{dt} &= \lambda S - (\mu + \omega)E, \\ \frac{dA}{dt} &= \eta\omega E - (\mu + \rho_3 + \nu_1 + u_2)A, \\ \frac{dI}{dt} &= (1 - \eta)\omega E - (\mu + \nu_2 + \nu_3)I, \\ \frac{dH}{dt} &= \nu_1A + \nu_2I + u_2A - (\rho_1 + \mu)H, \\ \frac{dJ}{dt} &= \nu_3I - (\mu + \rho_2)J, \\ \frac{dR}{dt} &= \rho_1H + \rho_2J + \rho_3A + u_1S - \mu R. \end{aligned} \tag{26}$$

The optimal control variables u_1 and u_2 minimise the objective function subject to model (26). The objective function is defined as:

$$J(u_1, u_2) = \min_{u_1, u_2} \int_0^{t_f} [A_1S(\tau) + A_2A(\tau) + B_1u_1^2(\tau) + B_2u_2^2(\tau)] d\tau, \tag{27}$$

where t_f is the fixed final time and the positive coefficients $A_1, A_2, B_1,$ and B_2 are constants that balance the cost and the

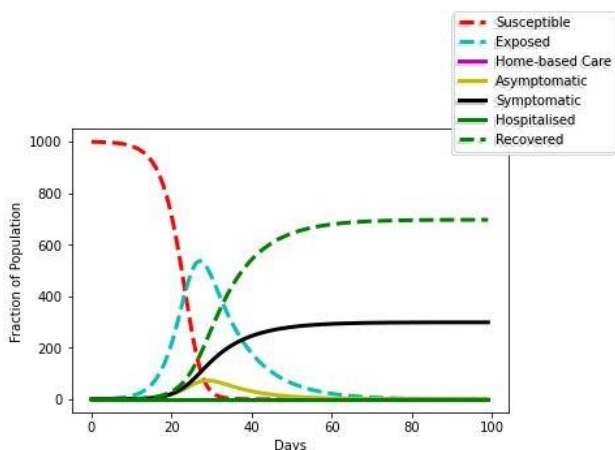


Figure 2. Absence of Interventions

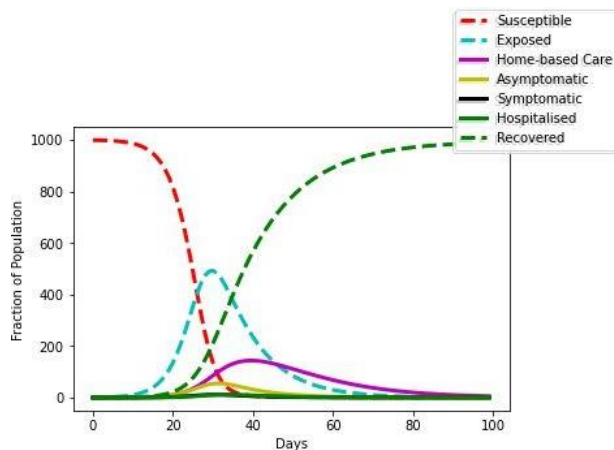


Figure 3. Presence of Interventions

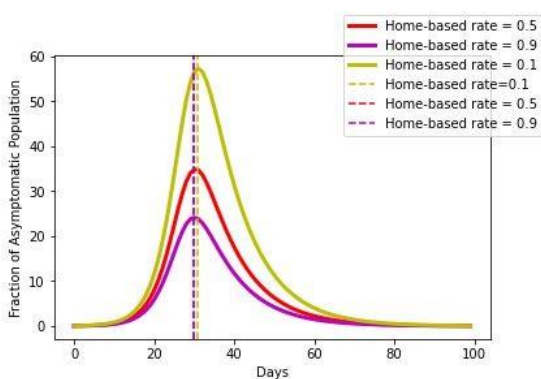


Figure 4. Effect of Home-based Care on Asymptomatics

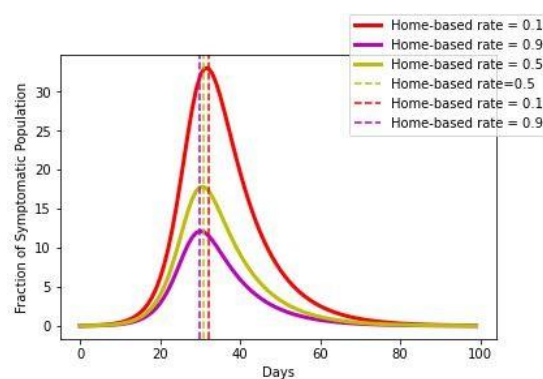


Figure 5. Effect of Home-based Care on Symptomatics

number of infected individuals at time t . In this paper, due to the non-linear measurement of control costs, we adopt the quadratic form commonly employed in [21, 22]. The primary objective is to determine the optimal control (u_1, u_2) such that

$$J(u_1^*, u_2^*) = \min (J(u_1, u_2) : u_1, u_2 \in U).$$

The controls u_1 and u_2 are assumed to be at least Lebesgue measurable on $[0, t_f]$ as described by the work of [23].

6.1. Existence of Optimal Control Problem

Theorem 7. The model (26) admits $u^* \in U_{ad}$ that verifies

$$J(u^*) = \min_{u \in U_{ad}} J(u).$$

Proof. To show the existence of an optimal control, we have to check the following assertions.

- The set of solutions to model (26) together with the initial condition and the corresponding control function in U_{ad} is nonempty.
- U_{ad} is closed and convex.
- The right-hand side of the proposed model is bounded by a linear function in control variables and the state.
- The Lagrangian $L(S, V, u_1, u_2)$ is convex on U_{ad} .

- There exist $\alpha_1 > 0$, $\alpha_2 > 0$, and $\rho > 1$ such that $L(S, A, u_1, u_2)$ satisfies

$$L(S, A, u_1, u_2) \geq \alpha_1 + \alpha_2(|v|^2 + |u|^2 + |w|^2)^\rho.$$

□

6.2. Characterisation of the optimal control

Now, to solve the optimal control problem model (26), we have constructed the Lagrangian equation as follows:

$$L(t, x, u) = \frac{dJ}{dt} = A_1 S(t) + A_2 A(t) + B_1 u_1^2(t) + B_2 u_2^2(t).$$

The necessary conditions that an optimal control should satisfy are derived from Pontryagin’s Maximum Principle [22, 24].

To minimize the Lagrangian, we have constructed the Hamiltonian equation by

$$H(t, x, u, \xi) = \frac{dJ}{dt} + \sum_{i=1}^7 P_i f_i = L(t, x, u) + \sum_{i=1}^7 P_i f_i,$$

where $L(t, x, u) = A_1 S + A_2 A + B_1 u_1^2(t) + B_2 u_2^2(t)$ and f_i , $i = 1, 2, 3, 4, 5, 6, 7$ are the right-hand side components of model (26).

The variables $P = (P_1, P_2, P_3, P_4, P_5, P_6, P_7) \in \mathbb{R}^7$ are costate variables associated with the state variables S, E, A, I, H, J and R , which can be determined from the second partial

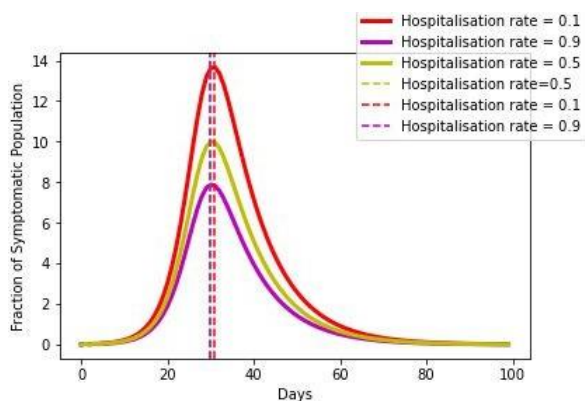


Figure 6. Effect of Hospitalisation on symptomatic

derivatives of H with respect to the state variables as follows:

$$\begin{aligned}
 H = & L(t, x, u) + P_1(\Lambda - (\lambda + \mu + u_1)S) \\
 & + P_2(\lambda S - (\mu + \omega)E) \\
 & + P_3(\eta\omega E - (\mu + \rho_3 + \gamma_1 + u_2)A) \\
 & + P_4((1 - \eta)\omega E - (\mu + \gamma_2 + \gamma_3)I) \\
 & + P_5(\gamma_1 A + \gamma_2 I - (\rho_1 + \mu)H) \\
 & + P_6(\gamma_3 I - (\mu + \rho_2)J) \\
 & + P_7(\rho_1 H + \rho_2 J + \rho_3 A + u_1 S - \mu R),
 \end{aligned}$$

where,

$$\begin{aligned}
 \frac{dP_1}{dt} &= -\frac{\partial H}{\partial S}, & \frac{dP_2}{dt} &= -\frac{\partial H}{\partial E}, & \frac{dP_3}{dt} &= -\frac{\partial H}{\partial A}, \\
 \frac{dP_4}{dt} &= -\frac{\partial H}{\partial I}, & \frac{dP_5}{dt} &= -\frac{\partial H}{\partial H}, & \frac{dP_6}{dt} &= -\frac{\partial H}{\partial J}, \\
 \frac{dP_7}{dt} &= -\frac{\partial H}{\partial R},
 \end{aligned}$$

thus,

$$\begin{aligned}
 \dot{P}_1 &= (\lambda + \mu + u_1)P_1 - P_2\lambda - P_7u_1, \\
 \dot{P}_2 &= (\mu + \omega)P_2 - \eta\omega P_3, \\
 \dot{P}_3 &= (\mu + \omega)P_3 - u_2P_5 - \rho - 3P_7, \\
 \dot{P}_4 &= (\mu + \gamma_2 + \gamma_3)P_4 - \gamma_2P_5 - \gamma_3P_6, \\
 \dot{P}_5 &= (\mu + \rho_1)P_5 - \rho_3P_6, \\
 \dot{P}_6 &= (\mu + \rho_2)P_6 - \rho_2P_7, \\
 \dot{P}_7 &= \mu P_7,
 \end{aligned}$$

with transversality conditions:

$$\begin{aligned}
 P_1(t_f) &= P_2(t_f) = P_3(t_f) = P_4(t_f), \\
 P_5(t_f) &= P_6(t_f) = P_7(t_f), \\
 L(t, x, u) &= \frac{1}{2}(B_1u_1^2 + B_2u_2^2).
 \end{aligned}$$

6.3. Optimal Control

The optimal controls u^*_1 and u^*_2 are found by solving,

$$\begin{aligned}
 \frac{\partial H}{\partial u_1} &= 0, \\
 \frac{\partial H}{\partial u_2} &= 0.
 \end{aligned}$$

Computing the partial derivatives of H with respect to u_1 and u_2

$$\frac{\partial H}{\partial u_1} = B_1U_1 - P_1S + P_7S,$$

setting,

$$\begin{aligned}
 \frac{\partial H}{\partial u_1} &= 0, \\
 B_1U_1 - P_1S + P_7S &= 0, \\
 (P_7S - P_1S) \frac{1}{B_1} &= u_1,
 \end{aligned}$$

similarly for u_2 ,

$$\frac{\partial H}{\partial u_2} = B_2U_2 - P_3A + P_5A,$$

setting,

$$\begin{aligned}
 \frac{\partial H}{\partial u_2} &= 0, \\
 B_2U_2 - P_3A + P_5A &= 0, \\
 (P_5A - P_3A) \frac{1}{B_2} &= u_2.
 \end{aligned}$$

Since, the controls u_1 and u_2 are bounded between 0 and 1, we use the projection operator,

$$\begin{aligned}
 u_1(t) &= \min\{1, \max\{0, u_{\Delta}\}\}, \\
 u_2(t) &= \min\{1, \max\{0, u_{\nabla}\}\},
 \end{aligned}$$

where:

$$\begin{aligned}
 u_{\Delta} &= \frac{P_7S - P_1S}{P_7S - P_1S}, \\
 u_{\nabla} &= \frac{P_5A - P_3A}{B_2}.
 \end{aligned}$$

The optimal control set $\{u^*(t), u^*(t)\}$ is given by:

$$\begin{aligned}
 u_1(t) &= \min_1 \left\{ 1, \max_0 \left\{ \frac{P_7S - P_1S}{P_7S - P_1S} \right\} \right\}, \\
 u_2(t) &= \min_2 \left\{ 1, \max_0 \left\{ \frac{P_5A - P_3A}{B_2} \right\} \right\}.
 \end{aligned}$$

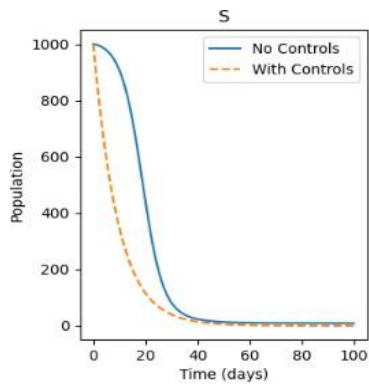


Figure 7. Susceptibles

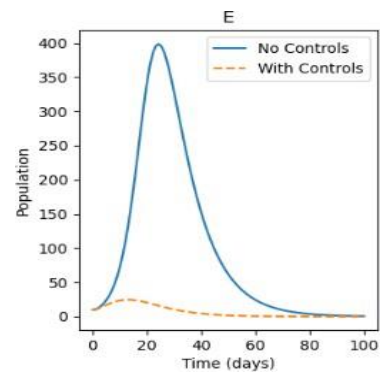


Figure 8. Exposed

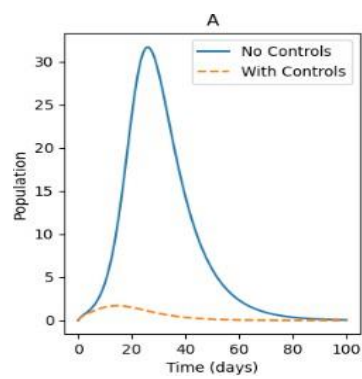


Figure 9. Asymptomatic

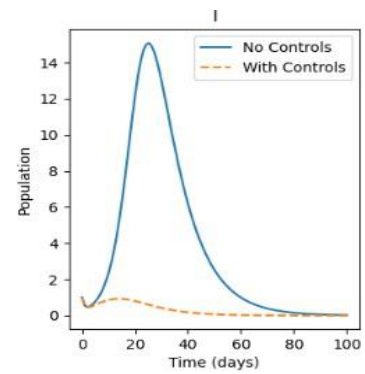


Figure 10. Symptomatic

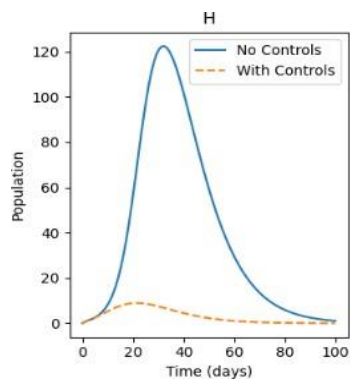


Figure 11. Home-based care

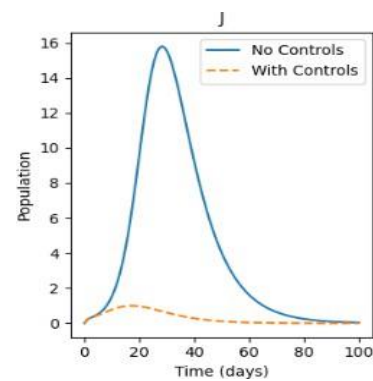


Figure 12. Hospitalisation

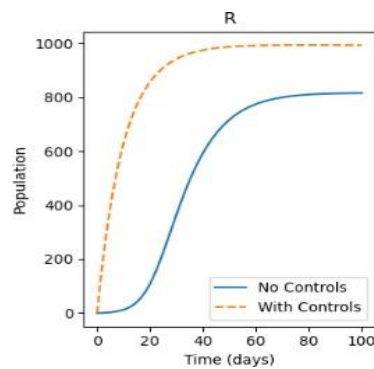


Figure 13. Recovered

6.4. Numerical Simulation of the Optimal Control Set

The epidemiological model presented here describes the dynamics of a population with respect to different compartments representing various stages of disease progression and intervention measures. Each curve in the plots represents the evolution over time of a specific compartment in the population. Here are the real-life meanings of each curve:

1. **S (Susceptible):** The graph presents the dynamics of a population under a disease model, specifically the SEAI (Susceptible, Exposed, Asymptomatic, Infected) compartments over a period of 100 days. Each subplot corresponds to a different compartment:
2. **S (Susceptible):** The population that is at risk of contracting the disease. Without controls, the susceptible population declines steeply, indicating a rapid spread of the disease. With controls, the decline is more gradual, suggesting that measures (e.g., vaccination, social distancing) are effective in reducing transmission.
3. **E (Exposed):** Individuals who have been exposed to the disease but are not yet symptomatic or infectious. Without controls, there is a sharp increase in the exposed population, peaking around day 20, followed by a decline. With controls, the peak is significantly lower and occurs slightly earlier, indicating that fewer people are getting exposed due to the implemented measures.
4. **A (Asymptomatic):** Individuals who are infected but do not show symptoms. The pattern is similar to the exposed group, with a sharp peak and decline without controls and a much lower peak with controls. This suggests that controls are effective in reducing asymptomatic infections.
5. **I (Infected):** Symptomatic and infectious individuals. Without controls, the infected population peaks around day 25, while with controls, the peak is much lower and occurs earlier. This indicates that controls help in managing symptomatic cases, reducing the burden on healthcare systems.
6. **H (Home-based Care):** Without controls, the Home-based care population peaks at around 120 individuals near day 25, indicating a significant healthcare burden. With controls, the peak is much lower, around 20 individuals, showing that interventions greatly reduce home-based care.
7. **J (Hospitalisations):** The hospitalised population peaks around 16 without controls and around 2 with controls, indicating that the disease's mortality is significantly mitigated by control measures.
8. **R (Recovered):** This curve shows the number of recovered individuals when control measures are applied. While controls might delay the number of new infections, eventually leading to fewer recoveries initially, it should ultimately lead to a higher number of recoveries by preventing deaths and severe cases.

Overall, the dashed lines ("With Controls") demonstrate that implementing control measures significantly flattens the curve across all compartments, highlighting the importance of interventions in managing disease spread.

7. Conclusion

This paper presents a deterministic model aimed at elucidating the effects of home-based care and hospitalisation on the

transmission dynamics of respiratory diseases. Through qualitative analyses, it has been demonstrated that these strategies can effectively curb the spread of infection, albeit temporarily, as more refined methods are under development. The paper underscores the importance of both home-based care and hospitalisation in managing infectious respiratory diseases. Home-based care serves as a valuable program, alleviating the strain on hospital resources and personnel by reserving them for severe cases. Additionally, it proves effective in reducing healthcare costs, allowing households to allocate resources to other essential needs such as food provision. However, it is noted that the feasibility of home-based care may be limited in lower-income households.

In summary, while home-based care is recommended as an interim measure, ongoing efforts to develop more comprehensive strategies are crucial.

Author Contributions. Wanjala, H. M.: Conceptualization, methodology, software validation, original draft preparation. Okongo, M. O.: review and editing, supervision. Ochwach, J. O.: review and editing, supervision.

Acknowledgement. The authors are thankful the editors and reviewers who have supported us in improving this manuscript.

Funding. This research received no external funding.

Conflict of interest. The authors declare no conflict of interest.

Data availability. The data used was mainly secondary data from published articles.

References

- [1] F. Brauer and C. Castillo-Chavez, "Mathematical models in population biology and epidemiology," vol. 2, no. 40, Springer, New York, 2012. DOI:10.1007/978-1-4614-1686-9
- [2] S. Chen *et al.*, "Curbing the COVID-19 pandemic with facility-based isolation of mild cases: a mathematical modeling study," *Journal of Travel Medicine*, vol. 28, no. 2, 2021. DOI:10.1093/jtm/taaa226
- [3] M. L. Ranney, V. Griffeth, and A. K. Jha, "Critical supply shortages—the need for ventilators and personal protective equipment during the Covid-19 pandemic," *New England Journal of Medicine*, vol. 382, no. 18, 2020. DOI:10.1056/NEJMp2006141
- [4] H. H. Elmousalami and A. E. Hassanien, "Day level forecasting for Coronavirus Disease (COVID-19) spread: analysis, modeling and recommendations," *arXiv preprint arXiv:2003.07778*, 2020.
- [5] T. Chakraborty and I. Ghosh, "Real-time forecasts and risk assessment of novel coronavirus (COVID-19) cases: A data-driven analysis," *Chaos, Solitons & Fractals*, vol. 135, p. 109850, 2020. DOI:10.1016/j.chaos.2020.109850
- [6] R. W. Mbogo and J. W. Odhiambo, "COVID-19 outbreak, social distancing and mass testing in Kenya—insights from a mathematical model," *Afrika Matematika*, vol. 32, no. 5-6, pp. 757–772, 2021. DOI:10.1007/s13370-020-00859-1
- [7] J. Panovska-Griffiths, "Can mathematical modelling solve the current Covid-19 crisis?," *BMC Public Health*, vol. 20, no. 1, p. 551, 2020. DOI:10.1186/s12889-020-08671-z
- [8] D. K. Gathungu *et al.*, "Modeling the effects of nonpharmaceutical interventions on COVID-19 spread in Kenya," *Interdisciplinary Perspectives on Infectious Diseases*, vol. 2020, pp. 1–10, 2020. DOI:10.1155/2020/6231461
- [9] A. R. Tuite, D. N. Fisman, and A. L. Greer, "Mathematical modelling of COVID-19 transmission and mitigation strategies in the population of Ontario, Canada," *Canadian Medical Association Journal*, vol. 192, no. 19, pp. E497–E505, 2020. DOI:10.1503/cmaj.200476
- [10] L. Mpinganzima *et al.*, "Compartmental mathematical modelling of dynamic transmission of COVID-19 in Rwanda," *IJID Regions*, vol. 6, pp. 99–107, 2023. DOI:10.1016/j.ijregi.2023.01.003

- [11] B. N. Kim *et al.*, "Mathematical model of COVID-19 transmission dynamics in South Korea: the impacts of travel restrictions, social distancing, and early detection," *Processes*, vol. 8, no. 10, p. 1304, 2020. DOI:10.3390/pr8101304
- [12] S. Mwalili *et al.*, "SEIR model for COVID-19 dynamics incorporating the environment and social distancing," *BMC Research Notes*, vol. 13, no. 1, p. 352, 2020. DOI:10.1186/s13104-020-05192-1
- [13] V. Ojiambo *et al.*, "A Human-Pathogen SEIR-P Model for COVID-19 Outbreak under different intervention scenarios in Kenya," *MedRxiv*, 2020. DOI:10.1101/2020.05.15.20102954
- [14] R. K. Titus, L. R. Cheruiyot, and C. P. Kipkurgat, "Mathematical modeling of Covid-19 disease dynamics and analysis of intervention strategies," *Mathematical Modelling and Applications*, vol. 5, no. 3, p. 176, 2020. DOI:10.11648/j.mma.20200503.16
- [15] I. M. Wangari *et al.*, "Mathematical modelling of COVID-19 transmission in Kenya: a model with reinfection transmission mechanism," *Computational and Mathematical Methods in Medicine*, vol. 2021, pp. 1–18, 2021. DOI:10.1155/2021/5384481
- [16] S. Olaniyi *et al.*, "Mathematical Modelling and Optimal Cost-Effective Control of COVID-19 Transmission Dynamics," *The European Physical Journal Plus*, vol. 135, no. 11, p. 938, 2020. DOI:10.1140/epjp/s13360-020-00954-z
- [17] H. M. Wanjala, "Mathematical Modelling of SARS-CoV-2 Incorporating Non-Pharmaceutical Interventions Coupled with Vaccination," Doctoral dissertation, Chuka University, 2023.
- [18] C. Connelly, "Epidemiology Through the Lens of Differential Equations," 2023.
- [19] R. K. MA, S. Sugiarto, and S. Nurwijaya, "Dynamical System for Tuberculosis Outbreak with Vaccination Treatment and Different Interventions on the Burden of Drug Resistance," *Jambura Journal of Biomathematics (JJBM)*, vol. 5, no. 1, pp. 10–18, 2020. DOI:10.37905/jjbm.v5i1.21903
- [20] R. S. Sihaloho and H. Nasution, "Dynamic analysis of SEIR model for Covid-19 spread in Medan," *Jambura Journal of Biomathematics (JJBM)*, vol. 3, no. 2, pp. 68–72, 2022. DOI:10.34312/jjbm.v3i2.16878
- [21] B. Pantha, F. B. Agosto, and I. M. Elmojtaba, "Optimal control applied to a visceral leishmaniasis model," *Electronic Journal of Differential Equations*, vol. 2020, no. 01-132, p. 80, 2020. DOI:10.58997/ejde.2020.80
- [22] Z. H. Shen *et al.*, "Mathematical modeling and optimal control of the COVID-19 dynamics," *Results in Physics*, vol. 31, p. 105028, 2021. DOI:10.1016/j.rinp.2021.105028
- [23] S. Lenhart and J. T. Workman, *Optimal control applied to biological models*, Chapman and Hall/CRC, 2007.
- [24] K. Dehingia *et al.*, "Dynamical behavior of a fractional order model for within-host SARS-CoV-2," *Mathematics*, vol. 10, no. 13, p. 2344, 2022. DOI:10.3390/math10132344
- [25] C. Castillo-Chavez, and B. Song, "Dynamical models of tuberculosis and their applications," *Mathematical Biosciences & Engineering*, vol. 1, no. 2, pp. 361–404, 2004. DOI:10.3934/mbe.2004.1.361
- [26] B. Buonomo and C. Vargas-De-León. "Stability and bifurcation analysis of a vector-bias model of malaria transmission," *Mathematical Biosciences*, vol. 242, no. 1, pp.59–67, 2013. DOI:10.1016/j.mbs.2012.12.001